

# Quantitative measurements of facets on the ulnar coronoid process from reformatted CT images

Guanyi Liu<sup>1#</sup>, Xianjing Zhao<sup>2,3#</sup>, Wei Wang<sup>3</sup>, Gang Chen<sup>2</sup>, Weihu Ma<sup>1</sup>, Jianming Chen<sup>1</sup>, Maosheng Xu<sup>2,3</sup>

<sup>1</sup>Department of Orthopedics Surgery, Ningbo 6th Hospital, Ningbo 315040, China; <sup>2</sup>The First Clinical Medical College, Zhejiang Chinese Medical University, Hangzhou 310053, China; <sup>3</sup>Department of Radiology, the 1st Affiliated Hospital of Zhejiang Chinese Medical University, Hangzhou 310006, China

<sup>#</sup>These authors contributed equally to this work.

*Correspondence to:* Maosheng Xu, MD. Department of Radiology, the 1st Affiliated Hospital of Zhejiang Chinese Medical University, 54 Youdian Road, Hangzhou 310006, China. Email: xums166@zcmu.edu.cn. Jianming Chen. Department of Orthopedics Surgery, Ningbo 6th Hospital, 1059 Zhongsandong Road, Ningbo 315040, China. Email: cjmdn01710@163.com.

**Background:** To quantify the size and angle of the medial and lateral facets of the ulnar coronoid process by reformatted computed tomography (CT) imaging.

**Methods:** Elbow CT images were retrospectively selected from the picture archiving and communication system in our hospital over a 5-year period (January 2011 to December 2015). The widths, heights, gradient and tilt angles of both the medial and lateral facet of the ulnar coronoid process were measured using two-dimensional (2D) reformations of CT images.

**Results:** Our database research yielded 120 elbow joints (53 right, 67 left) of 120 patients (54 males, 66 females) which fulfilled our criteria. The average width of the two facets of the ulnar coronoid process were  $13.34 \pm 1.85$  mm for the medial facet and  $8.39 \pm 1.29$  mm for the lateral facet. The average height of the medial facet was  $18.45 \pm 3.38$  mm and the lateral facet was  $17.55 \pm 3.81$  mm. The average tilt angles of medial and lateral facet were  $80.34^\circ \pm 7.71^\circ$  and  $98.78^\circ \pm 5.71^\circ$  respectively. The average gradient angles of the medial and lateral facet ridge were  $60.02^\circ \pm 8.78^\circ$  and  $36.97^\circ \pm 4.99^\circ$  respectively. The length of the lateral facet ridge was longer than the medial facet ridge.

**Conclusions:** Reformatted CT images allow for multiple, accurate measurements of facets on the ulnar coronoid process. These measurements can be applied to guiding appropriate surgical interventions for fractures in this area.

**Keywords:** Coronoid process; elbow; computed tomography (CT); anatomy

Submitted Apr 04, 2018. Accepted for publication May 31, 2018.

doi: 10.21037/qims.2018.06.02

View this article at: <http://dx.doi.org/10.21037/qims.2018.06.02>

## Introduction

The coronoid process of the ulna is an anterior extension of the proximal ulnar metaphysis. The ulnar coronoid process, along with its lateral and medial facets is a significant contributor to elbow stability. The lateral facet articulates with radial head and lateral trochlea of the humerus, whilst the medial facet articulates with medial trochlea. The

anterior bundle of the ulnar collateral ligament is attached to the sublime tubercle of medial facet (1,2). O'Driscoll *et al.* (3) proposed an extensive classification system based on fracture location and size. This system classifies coronoid fractures into coronoid tip fractures, anteromedial coronoid fractures, and basal coronoid fractures. The tip of coronoid process lies in the lateral facet, and a tip fracture generally results from the valgus (posterolateral) injury (3). On the other hand, an

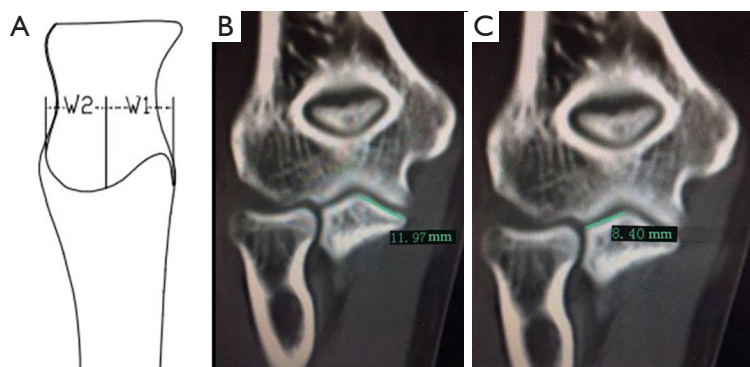


**Figure 1** The maximum widths of medial and lateral facets (W1, W2; A) in reformatted CT images (B,C).

anteromedial coronoid fracture affects the medial facet and generally results from varus (posteromedial) rotation or a shearing force. Fractures of the medial and lateral facets of the ulnar coronoid process have different mechanisms of injury and optimal strategies for treatment.

Although many anatomical studies emphasize the coronoid process of the ulna, they rarely focused on anatomic differences between the medial and lateral facets of the ulnar coronoid process (2,4-6). When fixing coronoid fractures, inappropriate insertion of screws into the facet of coronoid may protrude into the humeroulnar joint (7). Consequently, a reformatted CT scan of the ulnar coronoid process is helpful in understanding anatomic characteristics of the two facets and guiding appropriate treatment (8). We hypothesized that there are anatomic differences between the medial and lateral facets of coronoid process. The purpose of this study was to employ a reformatted two-dimensional (2D) CT imaging to accurately quantify differences of the size and angle between the medial and lateral facets of the ulnar coronoid process.

## Methods

Elbow CT images were retrospectively selected from the picture archiving and communication system (PACS, GE Medical systems, Milwaukee, WI, USA) within our hospital over a 5-year period (January 2011 to December 2015). Patients were selected for this study if their age ranged 18 to 60, and had no previous history of elbow lesions such as a deformity, fracture and tumor. The exclusion criterion was any failure to retrieve 2D reformatted images. Our Institutional Review Board approved the protocol for the use of these scans.

All CT scans were performed on a 64-slice CT scanner

(SOMATOM Sensation 64 or Definition AS, Siemens, Erlangen, Germany). Scan parameters were as follows: 120 kVp, 250 mAs, collimation: 0.6 mm  $\times$  64, field of view = 180 mm  $\times$  180 mm, matrix = 512  $\times$  512, rotation time = 0.33 s, routine slice thickness of 3 mm with an algorithm filter B70f for axial 2D interpretation and thin slice thickness of 0.75 mm with an algorithm filter B31f for coronal or sagittal 2D observation of elbow joint.

We conducted image manipulation using Syngo MultiModality Workplace. The reconstructed slice width was 0.75 mm and with a reconstruction increment of 0.4 mm. For each patient, reformatted 2D CT images were used to determine the sagittal and coronal plane for measurements. The sagittal plane was defined by 3 anatomic landmarks: at the most medial point of the coronoid facet, the point at the tip of the coronoid process and at the most lateral point of lesser sigmoid notch of the proximal ulna. The maximum widths of medial and lateral facets of the coronoid process were measured in the coronal plane (*Figure 1*). Measurements of two facets in reference to the sagittal plane included: (I) height with respect to the line representing maximum facet height (*Figure 2*) and to the maximum height of diaphysis of the ulna (*Figure 2*); (II) the tilt angle of facet (*Figure 3*); and (III) the gradient angle and length of facet ridge in the middle of the coronal plane (*Figures 4,5*).

In order to avoid bias for this morphometric study, measurements of two facets of the coronoid process were performed independently by 2 observers with over 10- years experience in CT diagnosis of musculoskeletal system, with accuracy of 0.1 mm and 0.1°. The interobserver reliability was calculated. In order to evaluate intra-observer reliability, each measurer repeated the measurements after a 2-week interval. The Pearson product-moment correlation coefficient ( $r$ ) was used to measure the level of intra-observer

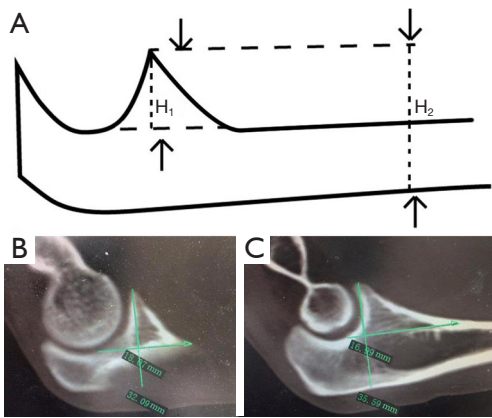


**Figure 2** The height with respect to the line representing maximum facet height and to the line representing the maximum ulna height (height of facet plus height of diaphysis of ulna) ( $H_1$ ,  $H_2$ ; A) in reformatted CT images (B,C).

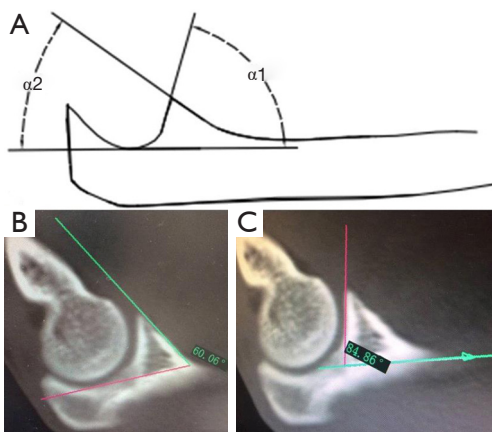


**Figure 3** The tilt angle of medial facet ( $\alpha_1$ , A) and gradient angle of medial facet ridge ( $\alpha_2$ ; A) in reformatted CT images (B,C).

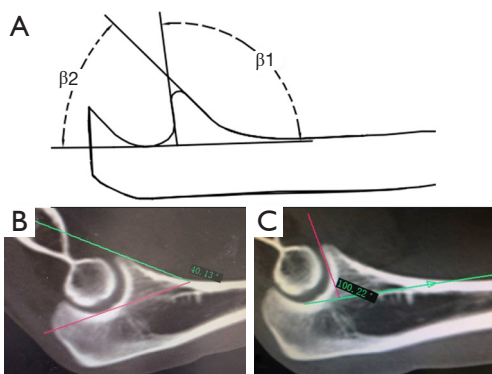


**Figure 4** The gradient angle of lateral facet ridge and tilt angle of lateral facet ( $\beta_1$ ,  $\beta_2$ ; A) in reformatted CT images (B,C).

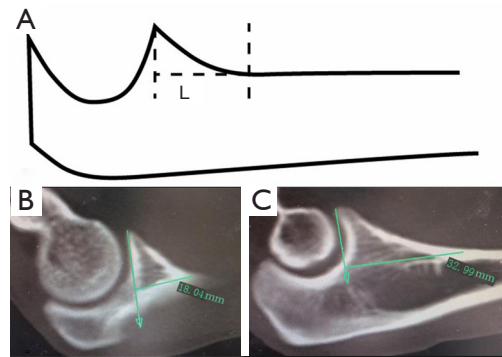


**Figure 5** The length of medial (A,B) and lateral (C) facet ridges in reformatted CT images.

**Table 1** Reliability of measurements

Parameter	r	P	Correlations
Width	0.92	<0.001	Excellent
Height	0.84	<0.001	Good
Total height	0.71	<0.001	Good
Tilt	0.77	<0.001	Good
Gradient	0.72	<0.001	Good
Length	0.87	<0.001	Good

and interobserver reliability for measurements of coronoid facets. Correlations between 0.70 and 0.89 were regarded as good and r values of 0.90 or greater were considered excellent (9). Results were averaged. All measurements were compared between left and right elbows of different patients, males and females, as well as medial and lateral facets. Two-sample test was conducted using SPSS software (version 12.0, SPSS Inc, Chicago, IL, USA). All results were shown as mean  $\pm$  standard deviation and a difference was considered to be statistically significant at  $P < 0.05$ .

**Results**

The measurement techniques had good or excellent intra-observer and interobserver reliability and the results of reliability of measurements were summarized in *Table 1*. Our database research yielded 120 elbow joints (53 right, 67 left) of 120 patients (54 males, 66 females) who fulfilled our criteria. The age range was from 22–60 years with a mean of 41 years. No significant differences between left and right elbows or between male and female controls were identified

**Table 2** Measurements of medial and lateral facets of the coronoid process between left and right elbows or between male and female controls ( $\bar{x} \pm S$ , n=120)

Parameter	Medial facet		Lateral facet		Medial facet		Lateral facet	
	Male (n=54)	Female (n=66)	Male (n=54)	Female (n=66)	Right (n=53)	Left (n=67)	Right (n=53)	Left (n=67)
Width (mm)	13.28±1.94	13.10±1.78	8.42±1.43	8.21±1.14	13.19±1.04	13.39±1.90	8.78±1.45	8.54±1.32
		t=-0.33, P=0.74			t=0.25, P=0.80	t=-0.39, P=0.71		t=0.35, P=0.69
Height (mm)	18.10±3.40	17.81±3.20	17.63±4.12	16.88±3.51	18.37±2.98	19.01±3.18	17.90±4.36	17.05±3.89
		t=-1.15, P=0.25			t=0.21, P=0.82	t=-0.91, P=0.30		t=0.45, P=0.58
Total height (mm)	30.05±2.28	29.73±2.43	34.49±3.09	33.77±2.58	29.87±2.19	29.80±2.78	35.42±4.01	36.10±3.21
		t=0.73, P=0.46			t=-0.52, P=0.59	t=0.74, P=0.47		t=-0.49, P=0.56
Tilt (°)	79.85±8.30	76.84±6.99	97.90±6.20	95.40±5.19	80.02±9.18	79.86±7.07	96.89±5.89	98.89±6.12
		t=-0.70, P=0.48			t=-0.47, P=0.63	t=-0.73, P=0.49		t=-0.70, P=0.48
Gradient (°)	61.01±8.08	59.89±7.98	36.89±4.08	35.02±4.45	68.13±7.98	64.20±8.01	36.78±4.52	35.89±5.32
		t=-0.56, P=0.70			t=-0.67, P=0.70	t=-0.69, P=0.56		t=-0.26, P=0.81
Length (mm)	23.58±2.09	22.71±2.40	22.98±2.63	22.66±2.87	22.69±2.23	23.58±2.39	23.78±2.15	24.31±3.24
		t=0.80, P=0.32			t=-0.48, P=0.79	t=0.76, P=0.42		t=-0.98, P=0.19

in the measurements (Table 2). The measurements of medial and lateral facets of the coronoid process were summarized in Table 3.

The medial facet was significantly wider than the lateral facet. Analysis of the average height of the two facets of the coronoid process demonstrated that although the medial facet was taller than the lateral facet, comparison of the height of the two facets revealed no statistically significant difference. However, a significant difference in height was found with respect to the line representing the maximal point of the ulnar height, with the lateral ulna measuring taller than medial ulna. The tilt angle of the medial facet is more acute than the lateral facet, and the lateral facet had a tendency to tilt to intra elbow joint. The gradient angle of the medial facet ridge was found to be steeper than the lateral ridge, and the lateral facet ridge formed relatively gentle slope during the transition to the distal end of the ulnar backbone. The length of the lateral facet ridge was significantly longer than the medial facet ridge.

### Discussion

The current study revealed that: (I) the medial facet of the ulnar coronoid process is wider and taller than the lateral facet; (II) the average tilt angles of the medial and lateral facets of the ulnar coronoid process were 80.34° and 98.78° respectively; (III) The medial and lateral facet ridges had different gradient angles and lengths.

Height and width measurements of the coronoid process varied in different studies (Table 4). Ablove *et al.* (4) measured 8 cadaveric specimens and found that the average height of coronoid process was 16.9 mm, while Cage and colleagues measured 18.3 mm in 20 cadaveric specimens (2). Separately, Matzon *et al.* (6) measured 15 mm in 35 cadaveric specimens. Doornberg and colleagues evaluated CT scans of 13 patients with the terrible-triad-pattern elbow injuries and concluded that the total height of the coronoid process of the ulna averaged around 19 mm (5). The width between the center axis of the trochlear notch and the most medial edge of the anteromedial facet averaged 12.5 mm (10). In our study, using a different method, we found an average width for the medial facet of the coronoid process of 13.34 mm, which was significantly wider than the lateral facet. Furthermore, the medial facet was taller than the lateral facet. Therefore, fractures of the medial facet often cause greater loss of articulation with the medial condyle of the humerus and may result in greater instability than fractures of the lateral facet (3,10,12). Although the

**Table 3** Measurements of medial and lateral facets of the coronoid process ( $\bar{x} \pm s$ , n=120)

Parameter	Medial facet	Lateral facet	Values
Width (mm)	13.34±1.85	8.39±1.29	t=23.96, P<0.01
Height (mm)	18.45±3.38	17.55±3.81	t=-1.92, P=0.055
Total Height (mm)	29.89±2.23	34.63±2.84	t=-14.04, P<0.001
Tilt (°)	80.34±7.71	98.78±5.71	t=-20.32, P<0.001
Gradient (°)	60.02±8.78	36.97±4.99	t=24.99, P<0.001
Length (mm)	23.74±2.53	32.31±1.90	t=-29.43, P<0.001

**Table 4** The review of previous studies of parameters of the coronoid process

Study	Year	Countries	Objects	Number	Parameter (mm)	
					Coronoid height	Coronoid width
Matzon (6)	2006	USA	CT	35	13–18	11–24
Doornberg (10)	2007	USA	Cadaver	21	8.7–20.1 (anteromedial)	1.7–5.4 (anteromedial)
Doornberg (5)	2006	USA	CT	13	12–25	–
Ablove (4)	2006	USA	Cadaver	8	13.9–19.5	–
Guitton (11)	2011	USA	CT	50	26±3.6	16±1.9

lateral facet was measured to be shorter than the medial facet, the height with respect to the line representing maximum ulnar height of lateral side (34.7 mm) was taller than medial side. The fact that the lateral facet is taller and covers the medial facet in the lateral radiographic view may be the reason why several Regan and Morrey type I fractures are categorized as severe anterior-medial coronoid process fractures (3,7,12-14). O'Driscoll *et al.* (3) introduced a classification scheme according to anatomic location and morphology of the fractures in reconstructions of CT scans. Fractures were divided into 3 types: type I fractures involve the tip, type II fractures involve the anteromedial facet, and type III fractures involve the basal aspect of the coronoid. These three types are further divided into subtypes based on the severity of coronoid involvement. The O'Driscoll's classification system improved our understanding of the lateral and medial facets of coronoid fracture. Large type I fracture fragments, type II and III fractures, especially those involving the anteromedial facet, should be treated surgically (3,15).

The medial and lateral facets of the ulnar coronoid process have different articular tilt angles and this may have certain clinical significance in the direction of screw insertion in order to avoid, or minimize intra-articular screw

placement. Measurements in our study found the tilt angle of the lateral facet is larger than the medial facet, suggesting that a screw inserted in lateral facet may more likely result in intra-articular screw placement. Since the average tilt angles of the medial facets were <90° and the angles of the lateral facets were the opposite, a vertical screw implant from the top of medial facet will not enter into the joint, but one in the lateral facet may (Figures 6, 7). Moreover, the tip of the lateral facet has a tendency to incline towards the joint. Reichel *et al.* (14) found "overhang" of the tip of coronoid process averaged 1.58 mm. Therefore, when fixing tip fractures, attention should be paid to increase tilt angles and avoid vertical insertion to prevent the screw from protruding into the humeroulnar joint.

Measurements of the facet ridges of the ulnar coronoid process have a certain clinical significance. Reichel *et al.* (14) identified three distinct ridges (medial, intermediate, lateral) on the coronoid process and measured their dimensions using 8 fresh frozen cadaveric elbows. They defined the lateral ridge as coursing along the anterior surface just medial to the lesser sigmoid notch; the medial ridge as running along the lateral edge of the sublime tubercle, and the intermediate ridge as the bone between the medial and lateral ridges. The average length of the medial ridge was



**Figure 6** The average tilt angles of the medial facets were  $<90^\circ$ , thus a vertical screw implant from the top of medial facet will not enter into the elbow joint.



**Figure 7** The average tilt angles of the lateral facets were  $>90^\circ$ , and the lateral facet had a tendency to tilt to intra elbow joint, thus a vertical screw implant from the top of lateral facet may enter into the elbow joint.

19.6 mm, the intermediate ridge measured 9.48 mm, and the lateral ridge was 15.1 mm (8). However, we found that the lateral ridge defined by Reichel *et al.* (14) was as part of sigmoid (radial) notch of the ulna and had less clinical significance with regard to elbow joint stability. Medial and lateral facet ridges were defined in the present study with a different view. The ridges began from the lateral and medial articular facets of the coronoid process and had different gradient angles and lengths. The medial facet ridge forms a steeper and shorter slope as it merges into the ulna compared to the lateral ridge. This means that a shear displacement of a medial facet fracture may be more unstable. If plating is to be performed, the plate should be properly shaped greater angle against the medial facet ridge than the lateral one.

Despite the strengths of this study, several limitations are worth noting. The sample size was limited to 120 elbow joints. This small sample size and the lack of repeated measurements may therefore preclude us from developing a comprehensive result. The ordinary CT reconstruction scans were used in the present work. To improve the validity of these findings, more intensive software packages for CT scans should be used in future investigations.

### Acknowledgements

We thank Dr. Quek Swee Tian from Department of

Diagnostic Imaging, National University Hospital for editing the manuscript.

*Funding:* This work was supported by the Natural Science Foundation of Ningbo City (grant numbers 2015A610216) and Ningbo Medical Science and Technology Project (grant numbers 2014A30).

### Footnote

*Conflicts of Interest:* The authors have no conflicts of interest to declare.

*Ethical Statement:* Our Institutional Review Board approved the protocol for the use of these scans (No. 2017-ZX-051-01).

### References

- Bellato E, Fitzsimmons JS, Kim Y, Bachman DR, Berglund LJ, Hooke AW, O'Driscoll SW. Articular Contact Area and Pressure in Posteromedial Rotatory Instability of the Elbow. *J Bone Joint Surg Am* 2018;100:e34.
- Cage DJ, Abrams RA, Callahan JJ, Botte MJ. Soft tissue attachments of the ulnar coronoid process. An anatomic study with radiographic correlation. *Clin Orthop Relat Res* 1995;(320):154-8.
- O'Driscoll SW, Jupiter JB, King GJ, Hotchkiss RN, Morrey BF. The unstable elbow. *Instr Course Lect* 2001;50:89-102.
- Ablove RH, Moy OJ, Howard C, Peimer CA, S'Doia S. Ulnar coronoid process anatomy: possible implications for elbow instability. *Clin Orthop Relat Res* 2006;449:259-61.
- Doornberg JN, van Duijn J, Ring D. Coronoid fracture height in terrible-triad injuries. *J Hand Surg Am* 2006;31:794-7.
- Matzon JL, Widmer BJ, Draganich LF, Mass DP, Phillips CS. Anatomy of the coronoid process. *J Hand Surg Am* 2006;31:1272-8.
- Iannuzzi NP, Paez AG, Parks BG, Murphy MS. Fixation of Regan-Morrey Type II Coronoid Fractures: A Comparison of Screws and Suture Lasso Technique for Resistance to Displacement. *J Hand Surg Am* 2017;42:e11-4.
- Mellema JJ, Janssen SJ, Guitton TG, Ring D. Quantitative 3-dimensional computed tomography measurements of coronoid fractures. *J Hand Surg Am* 2015;40:526-33.
- Pugh DM, Wild LM, Schemitsch EH, King GJ, McKee MD. Standard surgical protocol to treat elbow dislocations with radial head and coronoid fractures. *J Bone Joint Surg Am* 2004;86-A:1122-30.

10. Doornberg JN, de Jong IM, Lindenhovius AL, Ring D. The anteromedial facet of the coronoid process of the ulna. *J Shoulder Elbow Surg* 2007;16:667-70.
11. Guitton TG, Van Der Werf HJ, Ring D. Quantitative measurements of the coronoid in healthy adult patients. *J Hand Surg Am* 2011;36:232-7.
12. Ring D. Fractures of the coronoid process of the ulna. *J Hand Surg Am* 2006;31:1679-89.
13. Regan W, Morrey B. Fractures of the coronoid process of the ulna. *J Bone Joint Surg Am* 1989;71:1348-54.
14. Reichel LM, Milam GS, Hillin CD, Reitman CA. Osteology of the coronoid process with clinical correlation to coronoid fractures in terrible triad injuries. *J Shoulder Elbow Surg* 2013;22:323-8.
15. Weber MF, Barbosa DM, Belentani C, Ramos PM, Trudell D, Resnick D. Coronoid process of the ulna: paleopathologic and anatomic study with imaging correlation. Emphasis on the anteromedial "facet". *Skeletal Radiol* 2009;38:61-7.

**Cite this article as:** Liu G, Zhao X, Wang W, Chen G, Ma W, Chen J, Xu M. Quantitative measurements of facets on the ulnar coronoid process from reformatted CT images. *Quant Imaging Med Surg* 2018;8(5):500-506. doi: 10.21037/qims.2018.06.02